## SUPPLEMENTARY INFORMATION

**Supplementary Table 1 Predicted targets of NRMT based on M-(A/S/P)-P-K consensus.**

| Accession | Protein Name | N-term. sequence |
|---|---|---|
| **SPK** | | |
| CAA46340 | zinc-finger protein (ZNFpT17) | MSPKRDGLGT |
| NP_057463 | VCX - variable charge testis protein | MSPKPRASGP |
| NP_001260 | RCC1 - regulator of chromosome condensation 1 | MSPKRIAKRR |
| AAL86399 | transmembrane channel-like protein 1 | MSPKKVQIKV |
| **APK** | | |
| NP_000423 | slow cardiac myosin regulatory light chain 2 | MAPKKAKKRA |
| NP_524144 | fast skeletal myosin alkali light chain 1 | MAPKKDVKKP |
| CAG33244 | fast skeletal myosin light chain 2 | MAPKRAKRRT |
| NP_034989 | myosin, light chain 3 | MAPKKPEPKK |
| CAA36256 | myosin, light chain 4, alkali; atrial, embryonic | MAPKKPEPKK |
| NP_006800 | translocase of outer mitochondrial membrane 34 | MAPKFPDSVE |
| NP_783313 | NADH-ubiquinone oxidoreductase subunit | MAPKVFRQYW |
| NP_009038 | translocon-associated protein gamma subunit | MAPKGSSKQQ |
| NP_766513 | kelch-like protein 31 | MAPKKKTIKKN |
| BAD12560 | damage-specific DNA binding protein 2 | MAPKKRPETQ |
| NP_996879 | sperm associated antigen 17 | MAPKKEKGGT |
| AAW51946 | chemokine-like factor super family 2 | MAPKAAKGAK |
| NP_061149 | TCP11 | MAPKGILGSF |
| NP_000975 | ribosomal protein L23a | MAPKAKKEAP |
| AAI41841 | Mortality factor 4 like 1 | MAPKQDPKPK |
| NP_037490 | peptidylarginine deiminase type I | MAPKRVVQLS |
| NP_001472 | growth arrest-specific 8 | MAPKKKGKKG |
| AAD29855 | NAD+ ADP-ribosyltransferase 3 | MAPKPKPWVQ |
| NP_150092 | gamma-aminobutyric acid (GABA) A receptor | MAPKLLLLLC |
| AAL06239 | testis development protein NYD-SP29 | MAPKQKKKTS |
| NP_001116293 | SET | MAPKRQSPLP |
| NP_078782 | galactosidase, beta 1-like | MAPKKLSCLR |
| **PPK** | | |
| BAD97233 | X-prolyl aminopeptidase 1, soluble variant | MPPKVTSELL |
| NP_003753 | vesicle-associated membrane protein 4 | MPPKFKRHLN |
| AAO73048 | vaccinia related kinase 2 | MPPKRNEKYK |
| AAN64133 | retinoblastoma 1 | MPPKTPRKTA |
| NP_060941 | erythropoietin 4 immediate early response | MPPKKQAQAG |
| NP_001019 | ribosomal protein S25 | MPPKDDKKKK |
| NP_000967 | ribosomal protein L12 | MPPKFDPNEI |
| AAI27120 | XIRP1 protein | MPPKKKPQLP |
| NP_037473 | Obg-like ATPase 1 | MPPKKGGDGI |
| NP_002466 | smooth muscle/non-muscle myosin alkali light chain 6B | MPPKKDVPVK |

## SUPPLEMENTARY FIGURE LEGENDS

**Supplementary Figure 1. NRMT is highly conserved throughout evolution.**

**Supplementary Figure 2. Immunoprecipitated FLAG-NRMT methylates RCC1-His$_6$ on its N-terminal serine and SETα-FLAG immunoprecipitated from HeLa cells is methylated on its N-terminal alanine. a,** ETD MS/MS spectrum recorded on the $[M+4H]^{+4}$ ion (m/z 377.7) corresponding to the 13-residue, N-terminal peptide of rRCC1 (2-14 of the gene encoded sequence). This ETD spectrum confirms trimethylation of the α-N-terminal of the rRCC1-HIS$_6$ protein when incubated with FLAG-NMRT immunoprecipitated from Hela cells. The accurate mass measurement using an LTQ-FTMS, $377.2399^{+4}$, and calculated mass $377.2401^{+4}$ are within 0.5ppm (data not shown). Nominal masses for c'- and z'-type ions that are detected are shown above and below the peptide sequence. Ions in the spectrum are labeled accordingly. Unlabeled ions are caused by loss of small neutral molecules such as $H_2O$ and $NH_3$. Note that in addition to trimethylation of the alpha-N-terminal of rRCC1, mono- and dimethylation was also detected (data not shown). **b,** ETD MS/MS spectrum recorded on the $[M+5H]^{+5}$ ion (m/z 558.1) from a GluC generated SETα peptide (residues 1-25). This ETD spectrum confirms the presence of trimethylation of the α-N-terminal of the SETα protein. The accurate mass measurement using an LTQ-FTMS, $557.9283^{+5}$, and calculated mass $557.9297^{+5}$ are within 2.5 ppm (data not shown). Nominal masses for c'-type and z'-type ions that are detected are shown above and below the peptide sequence. Ions in spectrum are labeled accordingly. Unlabeled ions are caused by loss of small neutral molecules such as $H_2O$ and $NH_3$. Note that in addition to trimethylation of the α-N-terminal of the SETα protein, mono- and dimethylation was also detected (data not shown).

**Supplementary Figure 3. NRMT localization and stable viral knockdown lines. a**, Schematic of ELISA methylation assay. **b,** siRNA knockdown of NRMT in Hela cells significantly decreases NRMT, trimethylated RCC1, and SET (*) levels, as compared to control cells. Total RCC1 levels are not affected. β-catenin was used as a loading control. **c,** The control pGIPZ-shRNAmir lentivirus (expressing a hairpin against the 3' UTR of murine NRMT) does not decrease NRMT or methylated RCC1 levels as compared to untransfected cells. **d,** Human N- and C-terminally tagged NRMT-GFP express at the expected size (~50kD) and have no degradation products. **e,** NRMT-GFP expression in Hela cells shows predominantly nuclear localization. **f,** Dot blot of *in vitro* methylation assays showing the SPK peptide used in ITC experiments can be methylated by recombinant NRMT but the SPQ peptide cannot. Reactions with SPK or SPQ peptide alone or recombinant NRMT alone used as controls. **g,** Lentiviral knockdown of NRMT in HCT116 cells significantly decreases NRMT, dimethyl RCC1, trimethyl RCC1, and SET (*) levels, as compared to control cells. Total RCC1 levels are not affected. β-catenin was used as a loading control.

**Supplementary Figure 4. Identification of methylated proteins in mouse tissues**
**a**, Immunoblots of mouse tissue lysates using the anti-me2-PPK and anti-me3-SPK antibodies. Equal protein (20 μg) was loaded onto each lane. **b**, *In vitro* methylation reactions using mouse tissue lysates extracted with low (L) or high (H) salt as a source of methyltransferase activity. Recombinant human RCC1 was used as the substrate. Each reaction was split in two and

immunoblotted with anti-me2-SPK or anti-me3-SPK. + = HeLa nuclear extract, NL = no lysate, NS = no substrate. **c,** ETD MS/MS spectrrum of the methylated N-terminal peptide of kelch-like protein 31.

**Supplementary Figure 5. Schematic of the method used for the characterization of N-terminally modified peptides from immunopurified mouse heart- and spleen-derived proteins using liquid chromatography and mass spectrometry.**

**Supplementary Figures 6, 7, 8. Characterization of N-terminally di- or trimethylated peptides from mouse heart and spleen extracts using liquid chromatography and ETD mass spectrometry.** Data dependent single scan ETD MS/MS spectra were acquired in the ion trap of an FETD-enabled LTQ-Orbitrap hybrid instrument (Thermo Scientific, Bremen, Germany). Represented here are ETD spectra of the N-terminally modified peptides originating from multiple *Mus musculus* source proteins. For all spectra, the predicted monoisotopic singly and average doubly and triply charged c'- and z'$^{\cdot}$-type fragment ion masses are listed above and below the peptide sequence, respectively. The identified fragment ions are labeled in each spectrum and underlined within the peptide sequence. In all cases, ions corresponding to the precursor and those that fall within the 3 m/*z* isolation window are labeled with the ▼ symbol. Reduced charge species are labeled; ions corresponding to neutral losses from these species are represented by brackets. The spectra below represent ETD fragmentation of the N-terminally di- or trimethylated peptides from the indicated *Mus musculus* source proteins. **S6a,** Regulator of chromosome condensation, accession NP_598639 (me2-PPKRIAKRRSPPE, $[M+4H]^{+4}$ at m/*z* 390.74). **S6b,** SET translocation, accession NP_076360 (me3-APKRQSAILPQPKKPRPAAAPKLE, $[M+6H]^{+6}$ at m/*z* 440.11). **S7a,** Ribosomal protein L23a, accession NP_997406 (me3-APKAKKEAPAPPKAE, $[M+4H]^{+4}$ at m/*z* 394.49). **S7b**, Myosin, light polypeptide 2, regulatory, cardiac, slow, accession NP_034991 (me3-APKKAKKRIEGGSSNVFSMFEQTQIQE, $[M+5H]^{+5}$ at m/*z* 617.13). **S8,** Myosin, light polypeptide 3, accession NP_034989 (me3-APKKPEPKKDDAKAAAPK, $[M+4H]^{+4}$ at m/*z* 484.04).

**Supplementary Figure 9. RB nuclear localization and dynamics are not altered by α-N-terminal methylation. a,** Wild type RB-GFP and RB-GFP with a Lys4 to Gln mutation (K4Q) both localize to the nucleus in HCT116 cells. DNA is counterstained with DAPI. **b,** RB-FLAG localizes to the nucleus in both control and NRMT lentiviral knockdown HCT116 cell lines as shown by immunofluorescence with anti-FLAG antibody. DNA is counterstained with DAPI. **c,** FRAP of wild type and K4Q RB-GFP in nucleus of HCT116 cells. Error bars represent s.d. (n=7).

**Supplementary Fig. 1.**

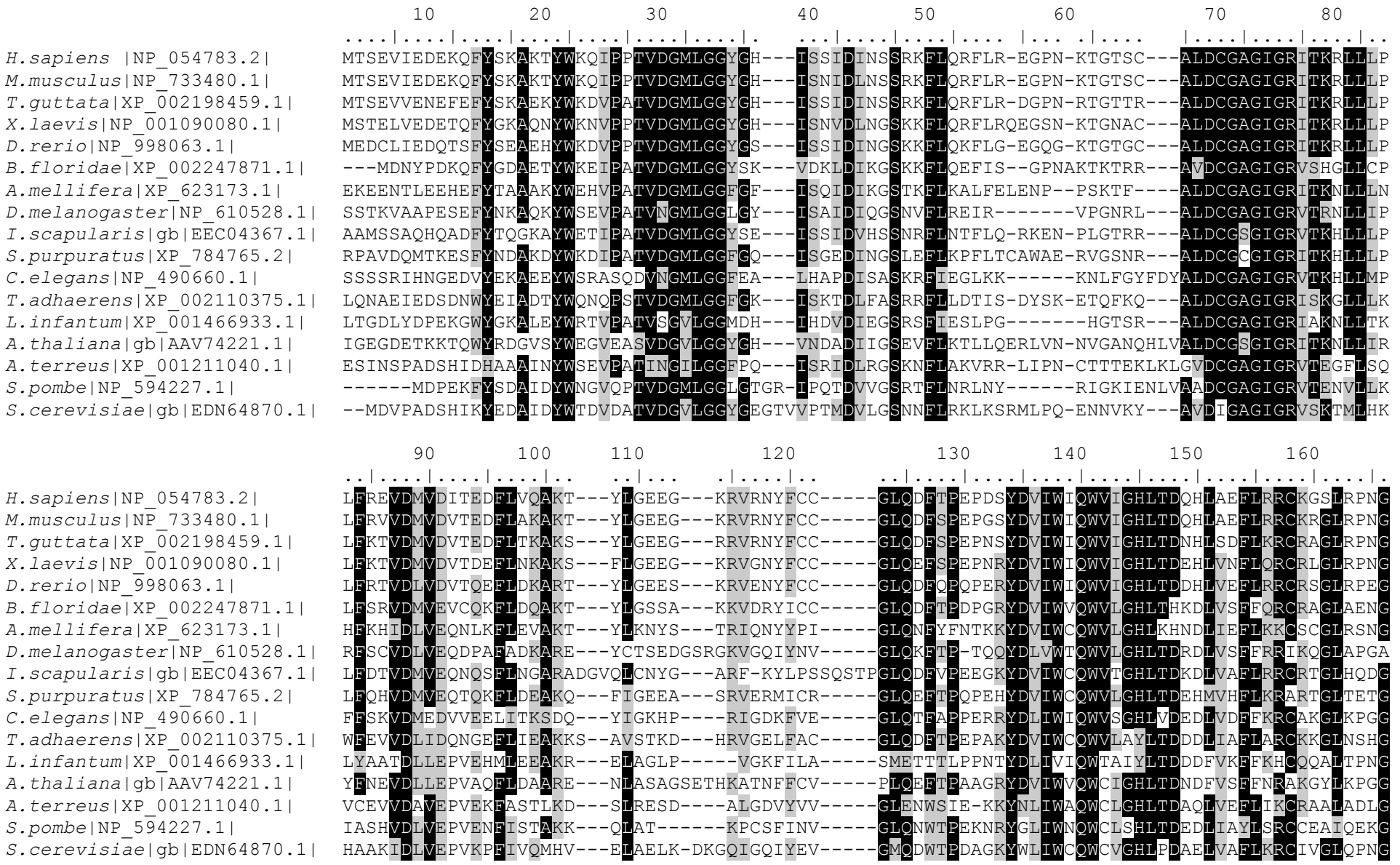

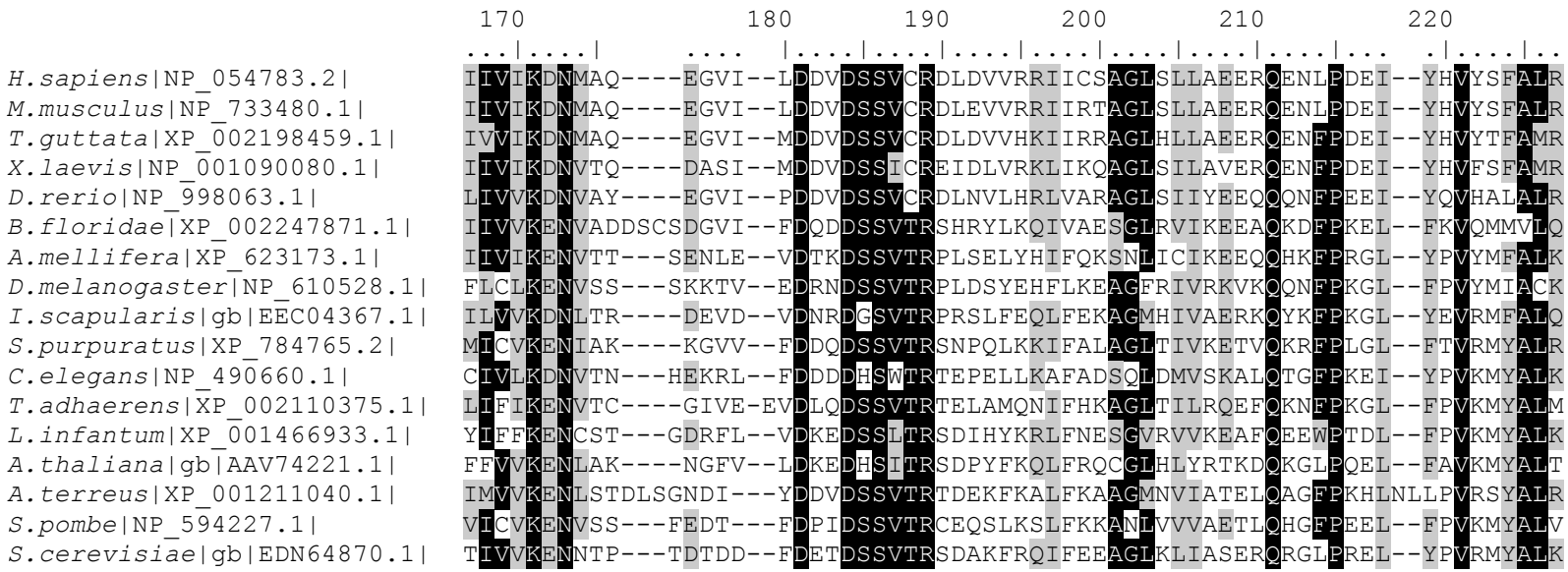
170
180
190
200
210
220
H.sapiens|NP_054783.2| IIVIKDNMAQ----EGVI--LDDVDSSVCRDLDVVRRIICSAGLSLLAEERQENLPDEI--YHVYSFALR
M.musculus|NP_733480.1| IIVIKDNMAQ----EGVI--LDDVDSSVCRDLEVVRRIIRTAGLSLLAEERQENLPDEI--YHVYSFALR
T.guttata|XP_002198459.1| IVVIKDNMAQ----EGVI--MDDVDSSVCRDLDVVHKIIRRAGLHLLAEERQENFPDEI--YHVYTFAMR
X.laevis|NP_001090080.1| IIVIKDNVTQ----DASI--MDDVDSSICREIDLVRKLIKQAGLSILAVERQENFPDEI--YHVFSFAMR
D.rerio|NP_998063.1| LIVVKDNVAY----EGVI--PDDVDSSVCRDLNVLHRLVARAGLSIIYEEQQQNFPEEI--YQVHALALR
B.floridae|XP_002247871.1| IIVVKENVADDSCSDGVI--FDQDDSSVTRSHRYLKQIVAESGLRVIKEEAQKDFPKEL--FKVQMMVLQ
A.mellifera|XP_623173.1| IIVIKENVTT---SENLE--VDTKDSSVTRPLSELYHIFQKSNLICIKEEQQHKFPRGL--YPVYMFALK
D.melanogaster|NP_610528.1| FLCLKENVSS---SKKTV--EDRNDSSVTRPLDSYEHFLKEAGFRIVRKVKQQNFPKGL--FPVYMIACK
I.scapularis|gb|EEC04367.1| ILVVKDNLTR----DEVD--VDNRDGSVTRPRSLFEQLFEKAGMHIVAERKQYKFPKGL--YEVRMFALQ
S.purpuratus|XP_784765.2| MICVKENIAK----KGVV--FDDQDSSVTRSNPQLKKIFALAGLTIVKETVQKRFPLGL--FTVRMYALR
C.elegans|NP_490660.1| CIVLKDNVTN---HEKRL--FDDDDHSWTRTEPELLKAFADSQLDMVSKALQTGFPKEI--YPVKMYALK
T.adhaerens|XP_002110375.1| LIFIKENVTC----GIVE-EVDLQDSSVTRTELAMQNIFHKAGLTILRQEFQKNFPKGL--FPVKMYALM
L.infantum|XP_001466933.1| YIFFKENCST---GDRFL--VDKEDSSLTRSDIHYKRLFNESGVRVVKEAFQEEWPTDL--FPVKMYALK
A.thaliana|gb|AAV74221.1| FFVVKENLAK----NGFV--LDKEDHSITRSDPYFKQLFRQCGLHLYRTKDQKGLPQEL--FAVKMYALT
A.terreus|XP_001211040.1| IMVVKENLSTDLSGNDI---YDDVDSSVTRTDEKFKALFKAAGMNVIATELQAGFPKHLNLLPVRSYALR
S.pombe|NP_594227.1| VICVKENVSS---FEDT---FDPIDSSVTRCEQSLKSLFKKANLVVVAETLQHGFPEEL--FPVKMYALV
S.cerevisiae|gb|EDN64870.1| TIVVKENNTP---TDTDD--FDETDSSVTRSDAKFRQIFEEAGLKLIASERQRGLPREL--YPVRMYALK

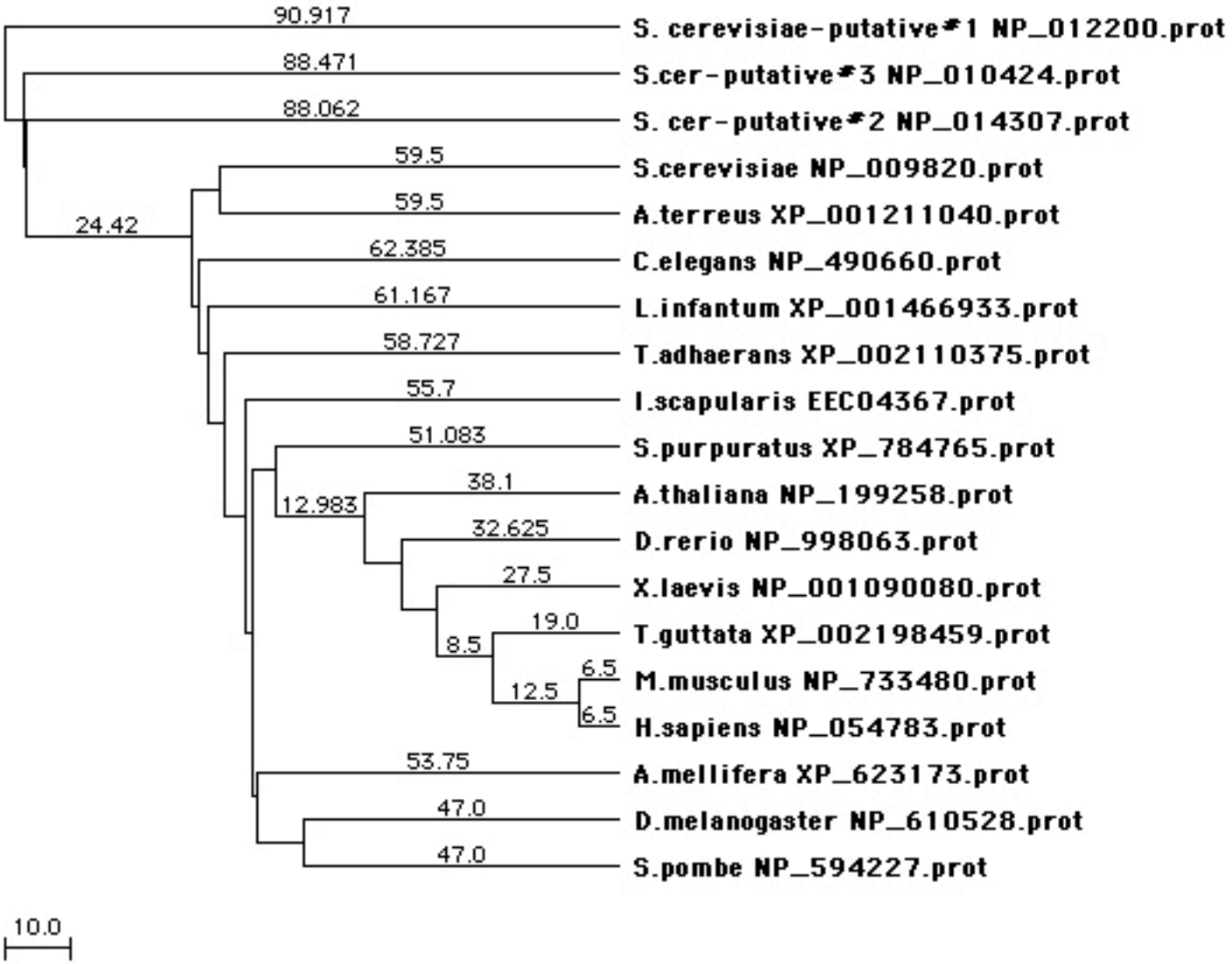
90.917
S. cerevisiae-putative#1 NP_012200.prot
88.471
S.cer-putative#3 NP_010424.prot
88.062
S. cer-putative#2 NP_014307.prot
59.5
S.cerevisiae NP_009820.prot
59.5
A.terreus XP_001211040.prot
24.42
62.385
C.elegans NP_490660.prot
61.167
L.infantum XP_001466933.prot
58.727
T.adhaerans XP_002110375.prot
55.7
I.scapularis EEC04367.prot
51.083
S.purpuratus XP_784765.prot
38.1
12.983
A.thaliana NP_199258.prot
32.625
D.rerio NP_998063.prot
27.5
X.laevis NP_001090080.prot
19.0
8.5
T.guttata XP_002198459.prot
6.5
12.5
M.musculus NP_733480.prot
6.5
H.sapiens NP_054783.prot
53.75
A.mellifera XP_623173.prot
47.0
D.melanogaster NP_610528.prot
47.0
S.pombe NP_594227.prot
10.0

Supplementary Figure 2. Tooley et al.

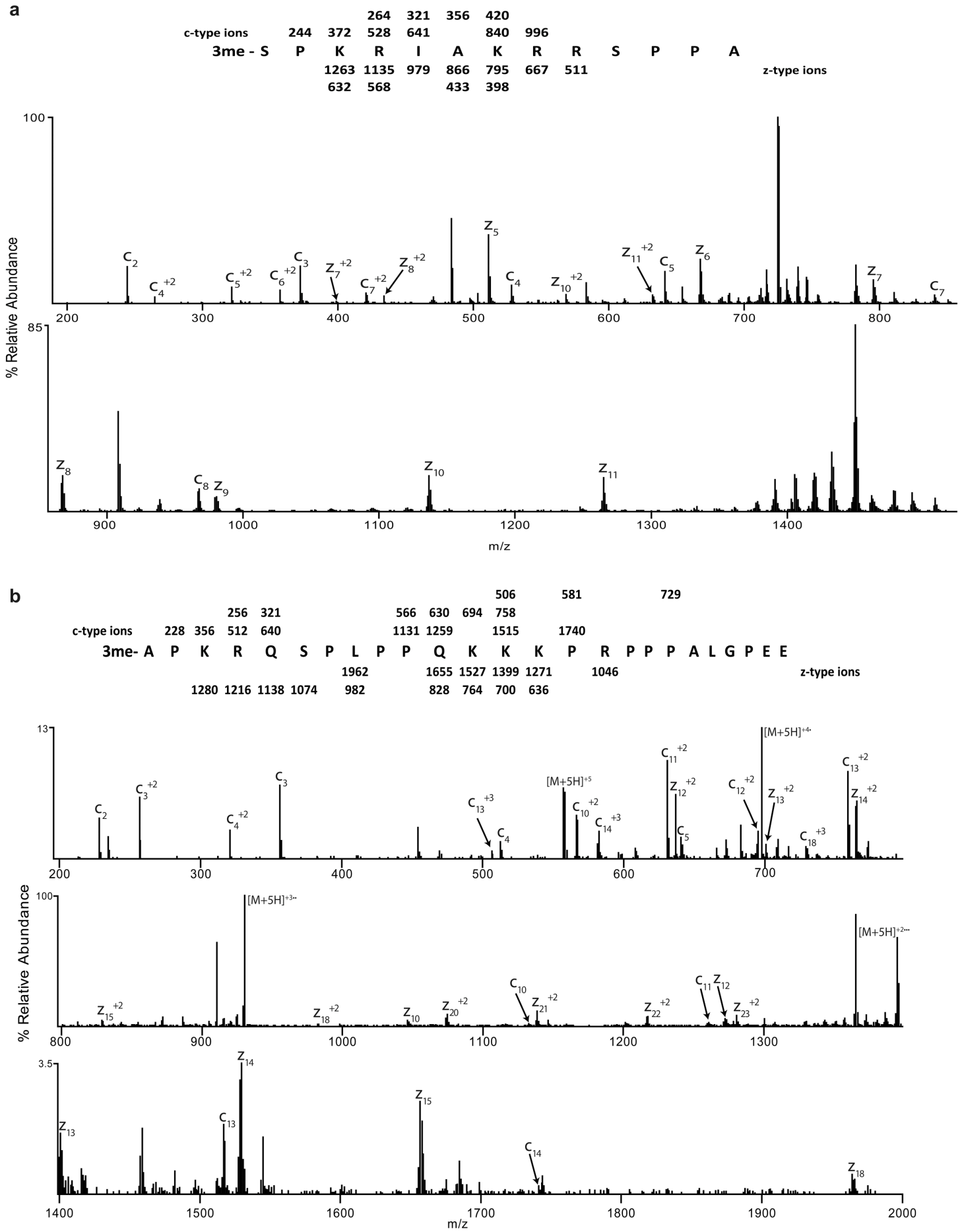

Supplementary Figure 3. Tooley et al.

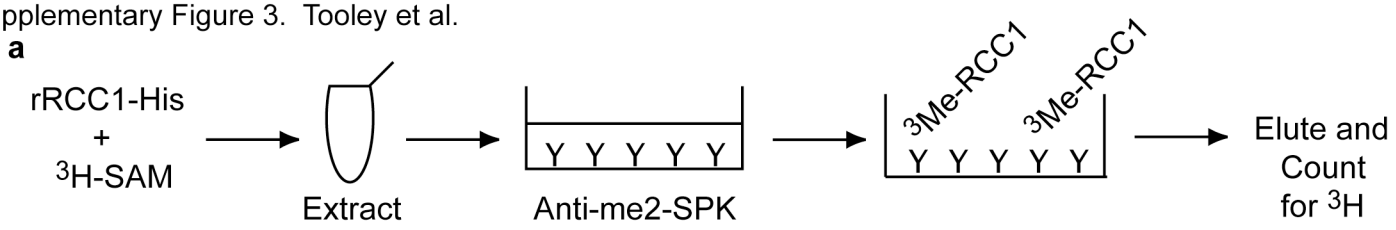


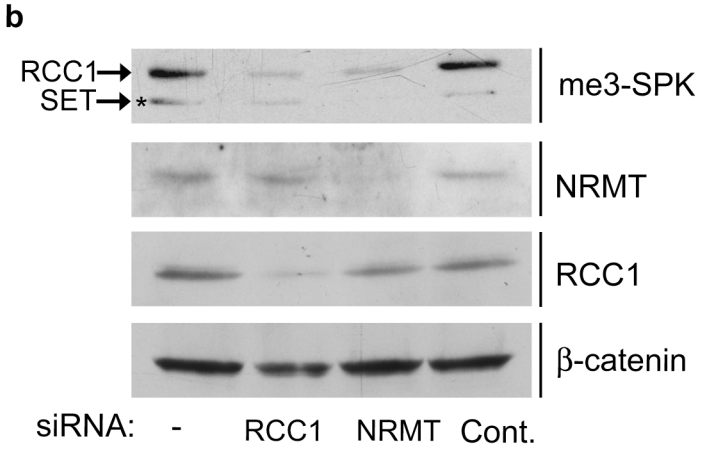


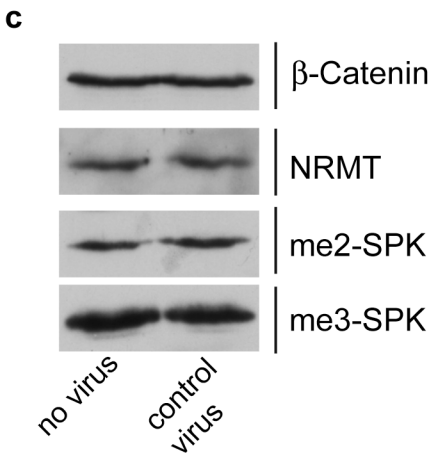


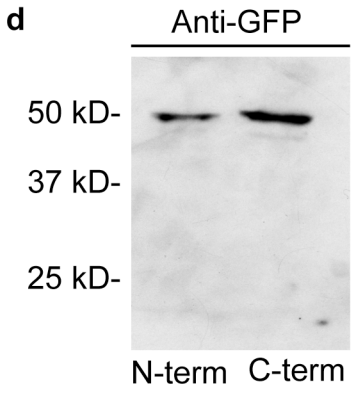


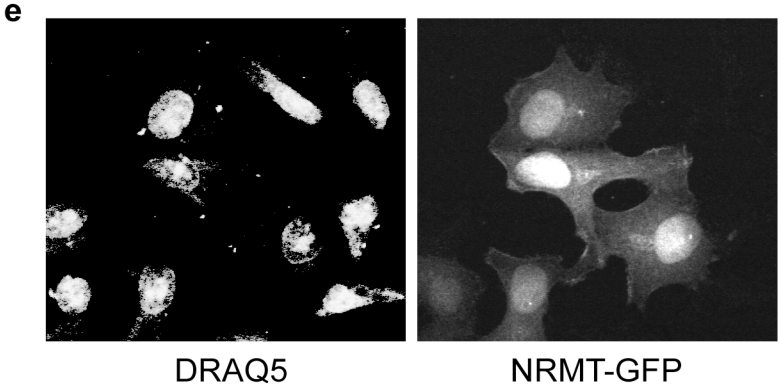


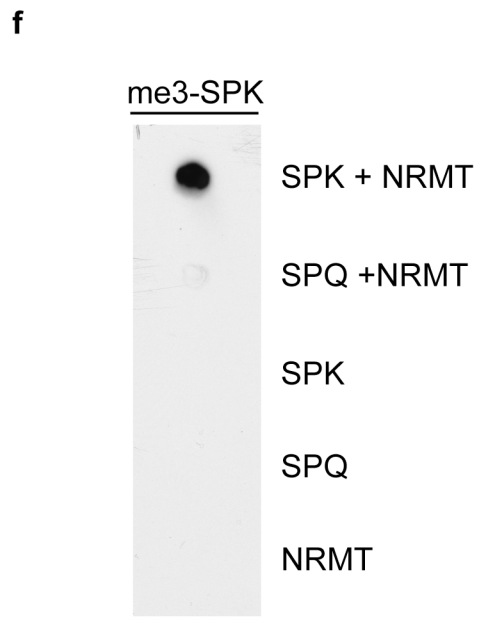


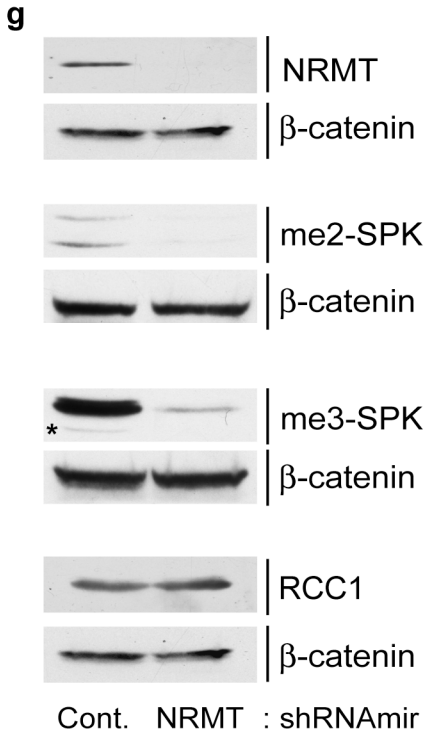

Supplementary Fig S4 Tooley et al.

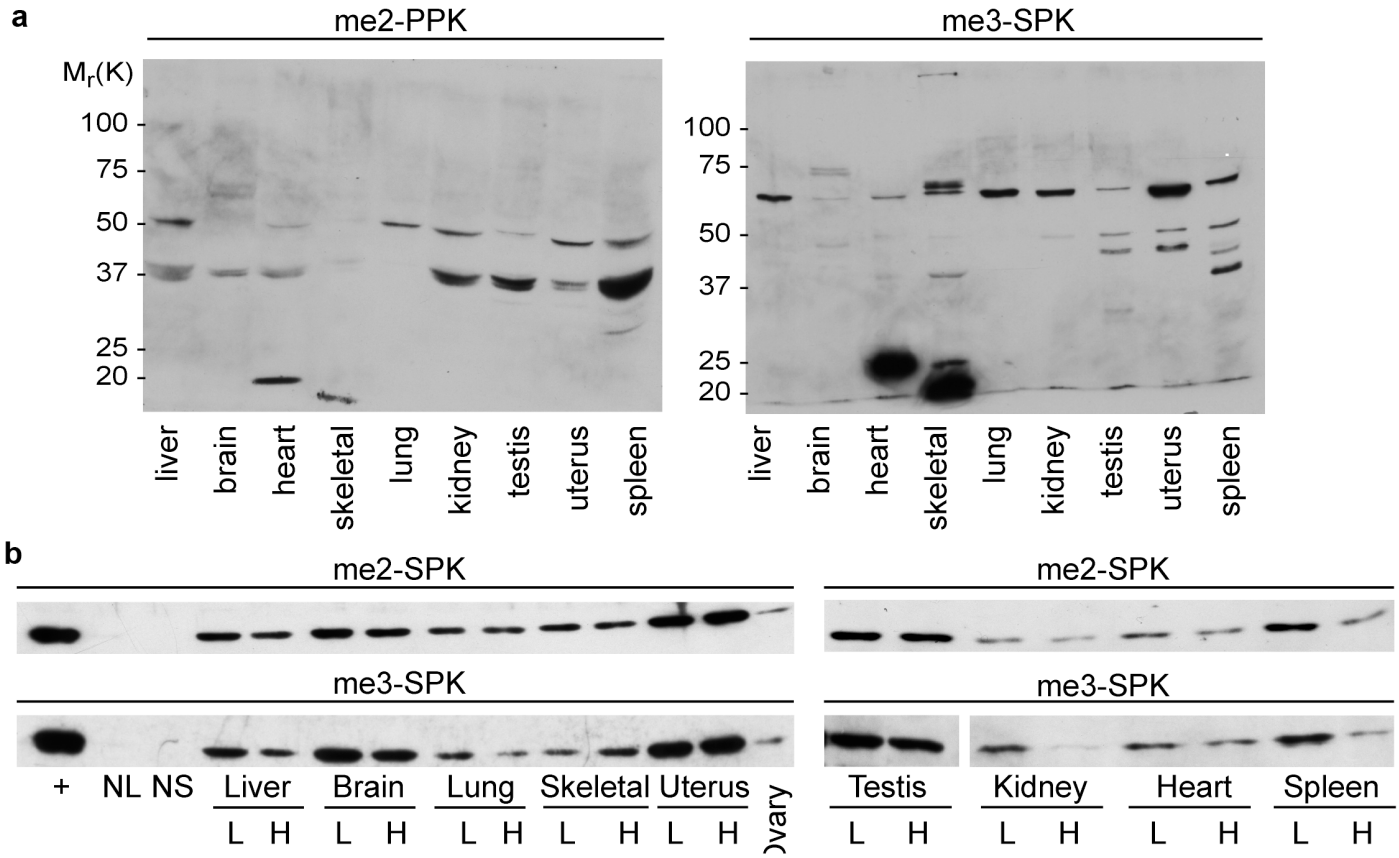


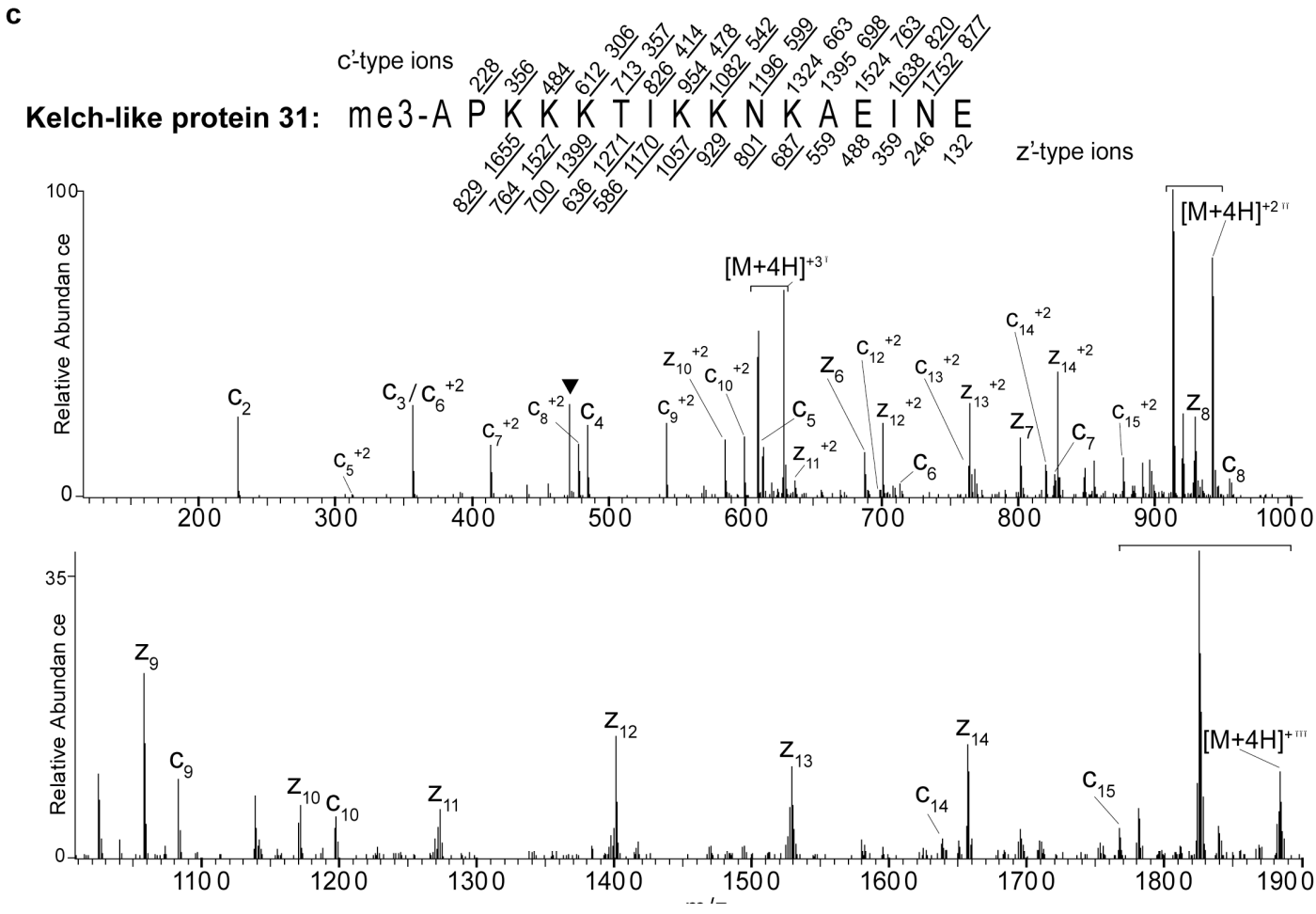

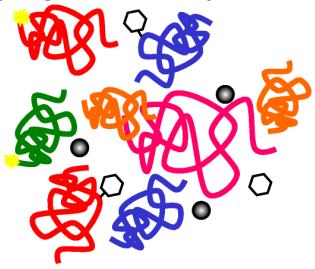

Mouse heart/spleen tissue lysate

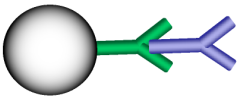

Agarose beads coupled to
Protein A/G and anti-me3-SPK
for immunoprecipitation

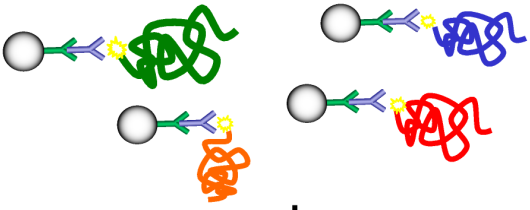

1. Reduction and carbamidomethylation
of Cys residues

2. Endoproteinase Asp-N and Glu-C
on-bead digestion

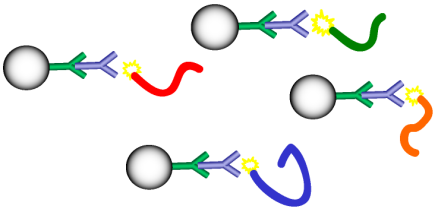

N-terminus-containing, modified peptides
bound to antibody remain on beads

+

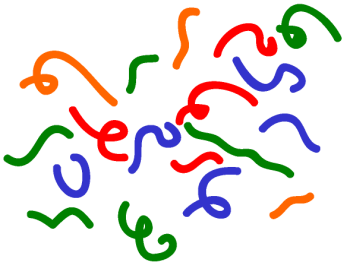

Asp-N/Glu-C generated peptides

LC- CAD &
ETD MS

Source Protein Identification

Spin column
with MW filter

Wash beads with
pH 2.8 elution buffer

Centrifuge at 3000 x g

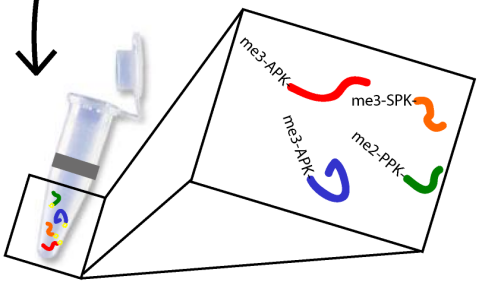


LC-CAD/ETD MS

me3 - APKKKTIKKNKAEINE

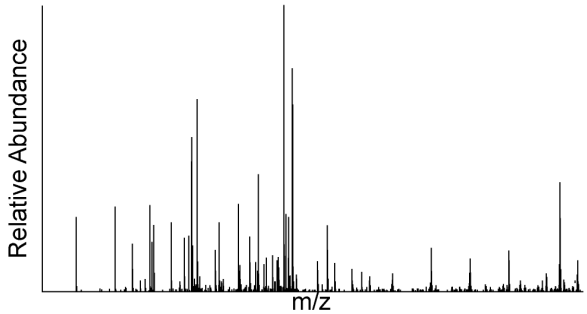


Modified Peptide Characterization

Supplementary Fig. 6. Tooley et al.

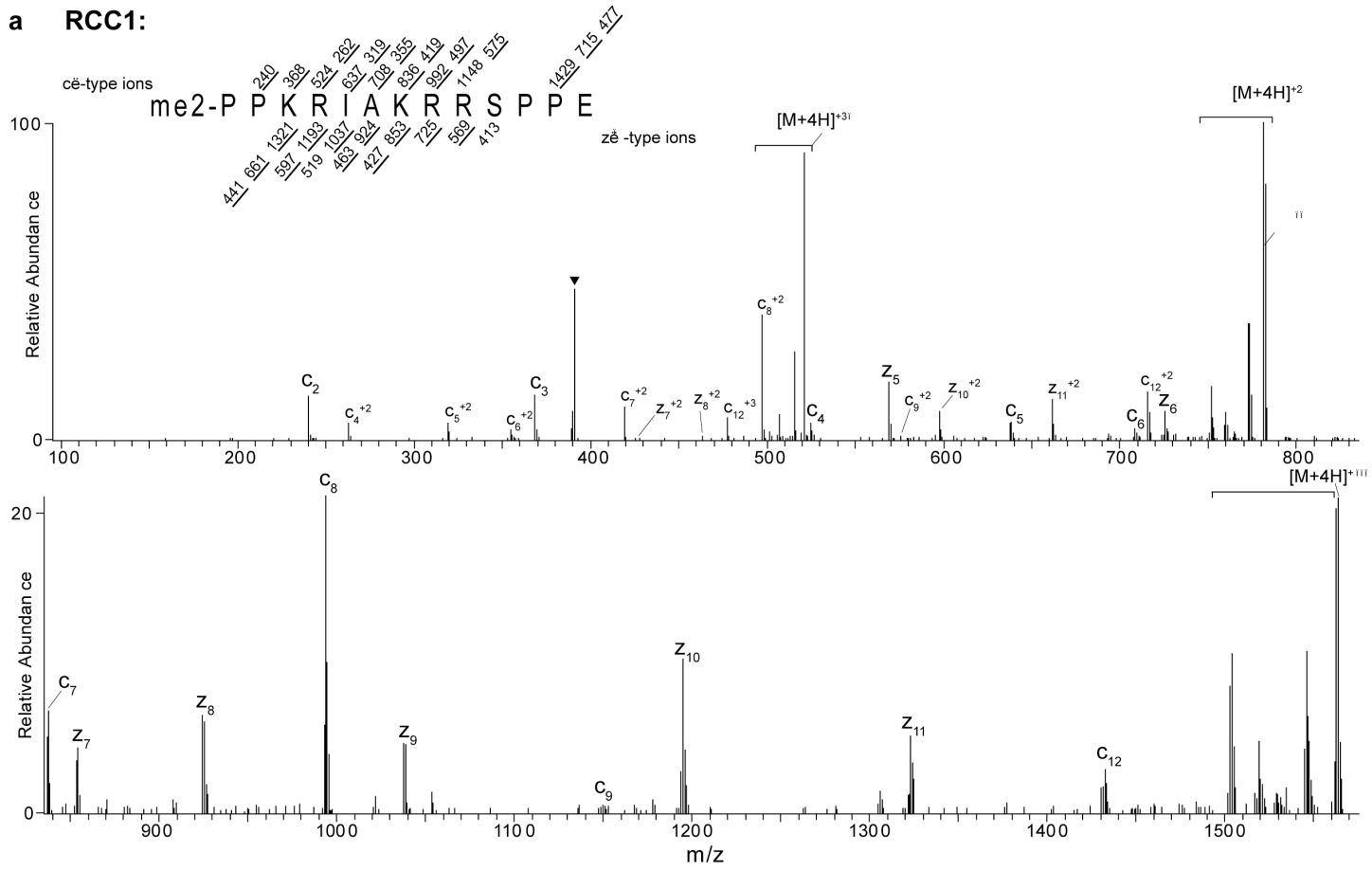


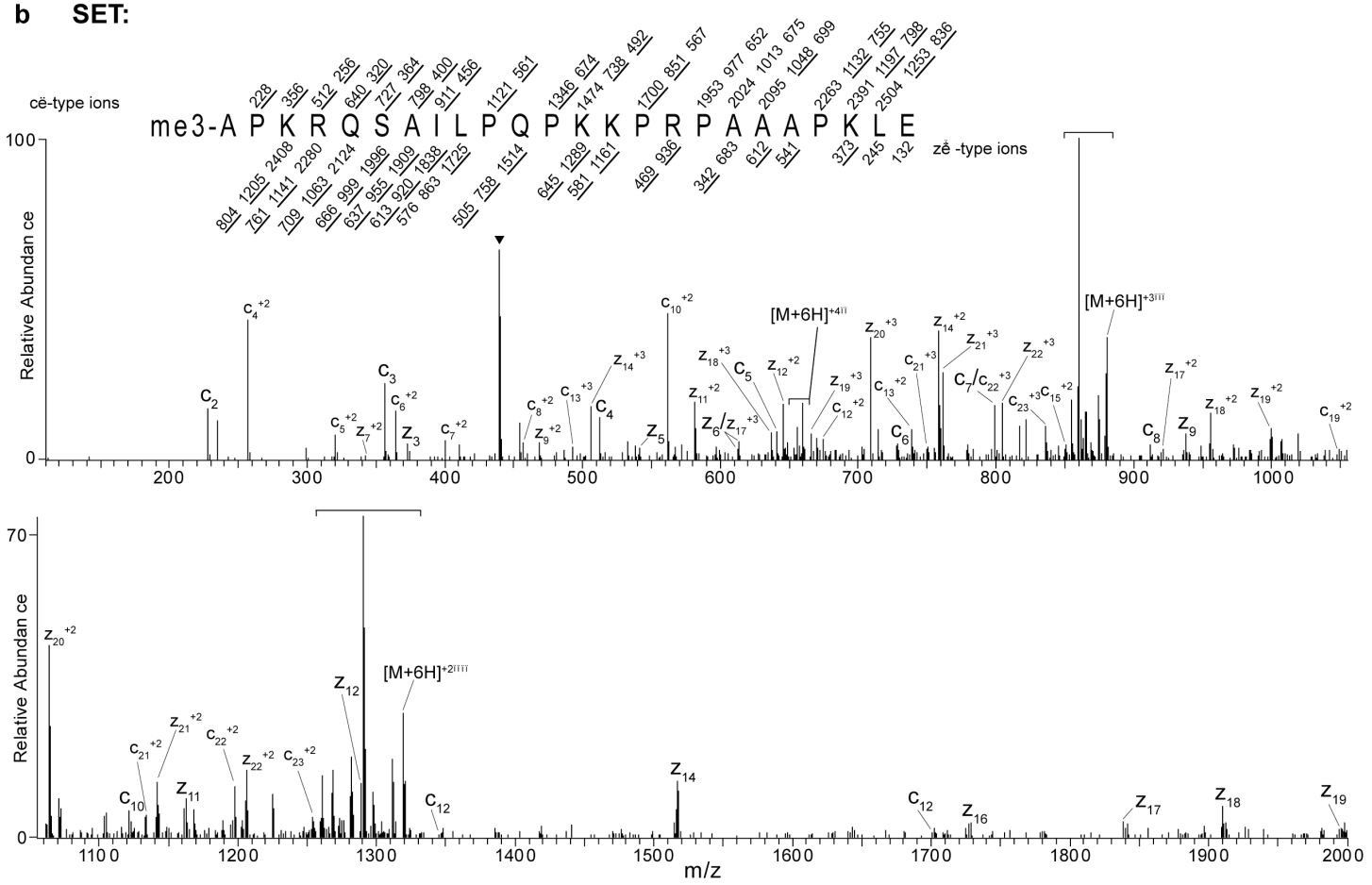

Supplementary Fig S7 Tooley et al.

**a Ribosomal protein L23a**

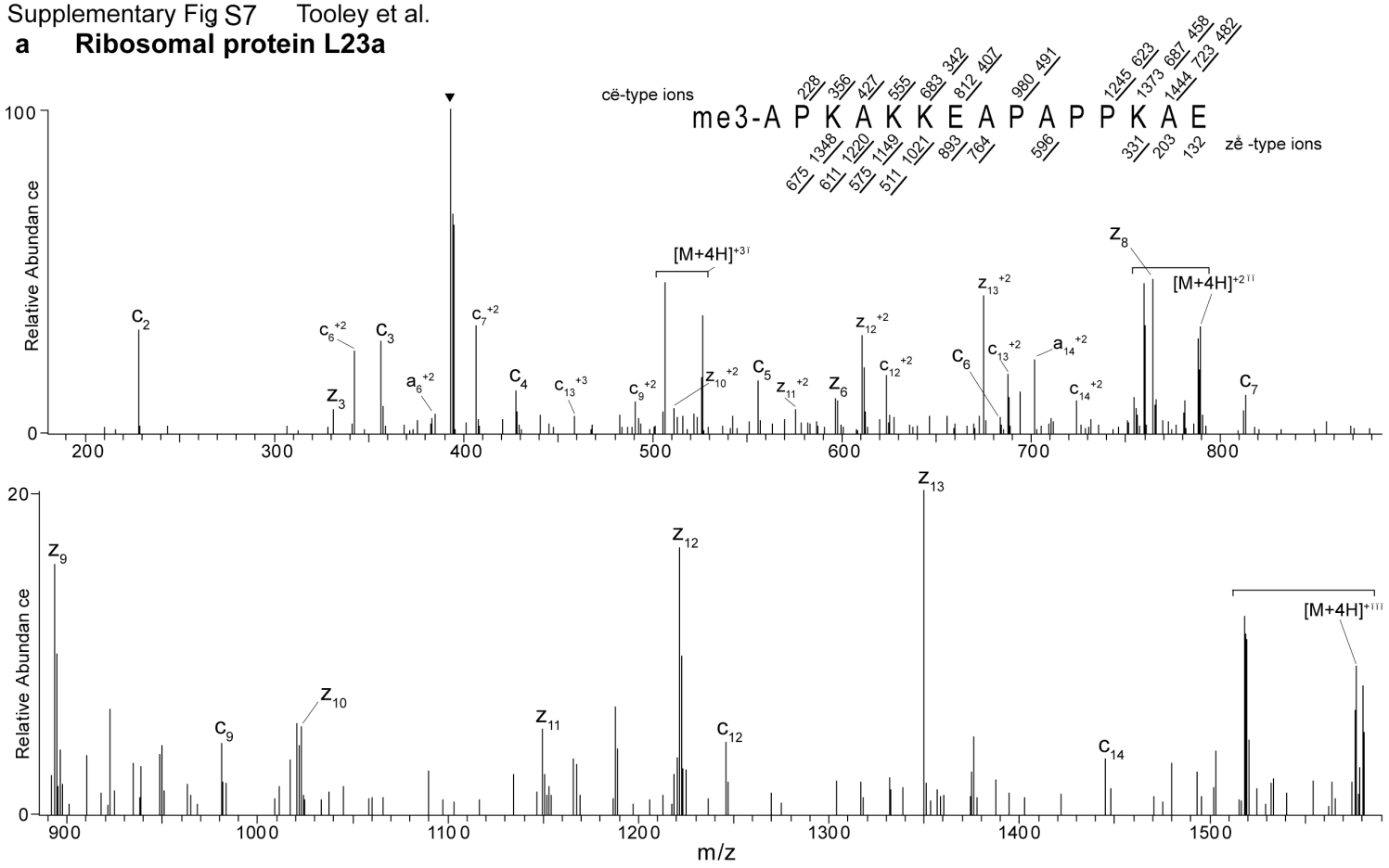


**b Myosin light chain 2:**

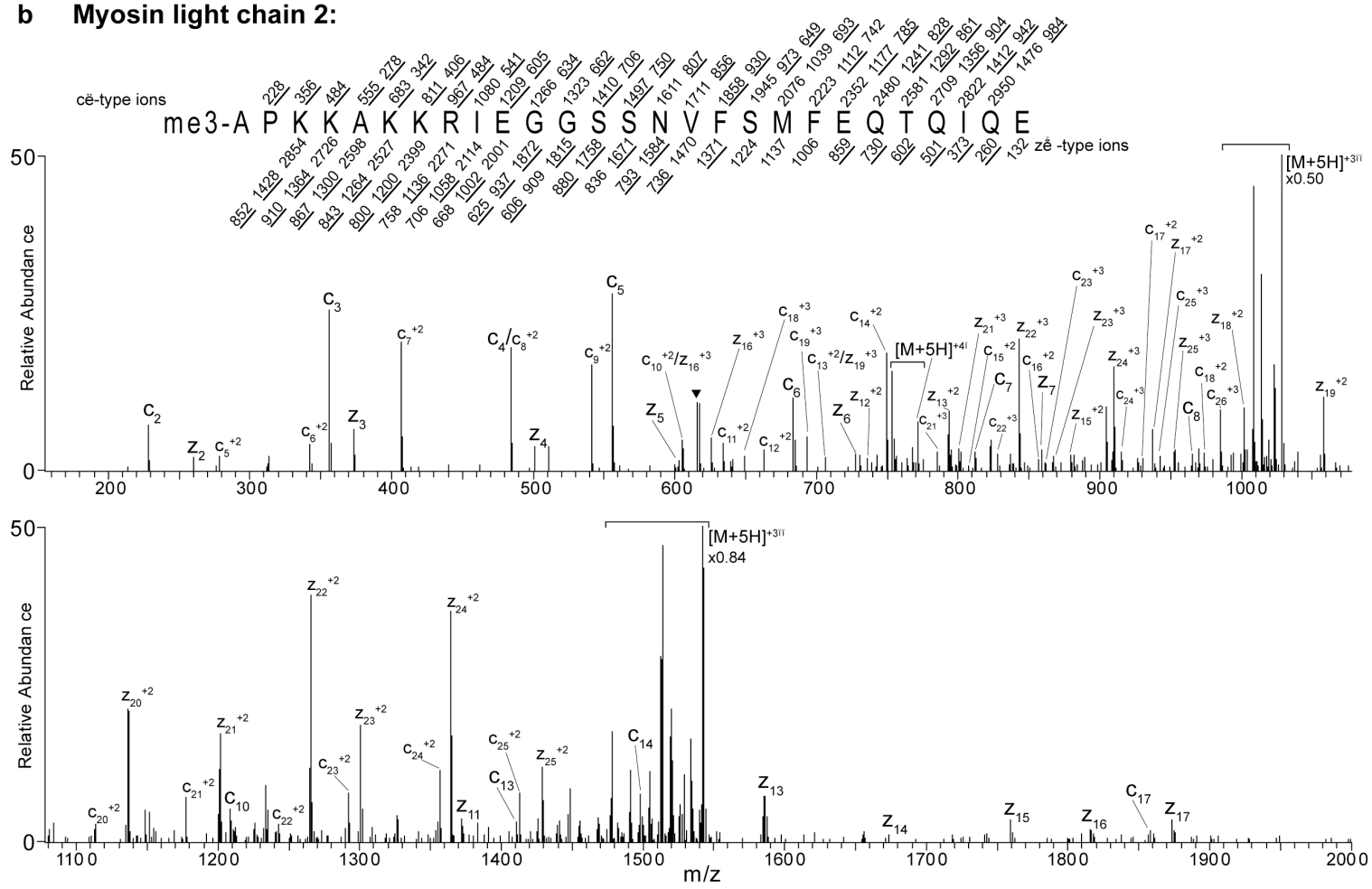

Supplementary Fig S8 Tooley et al.

**Myosin light chain 3:**

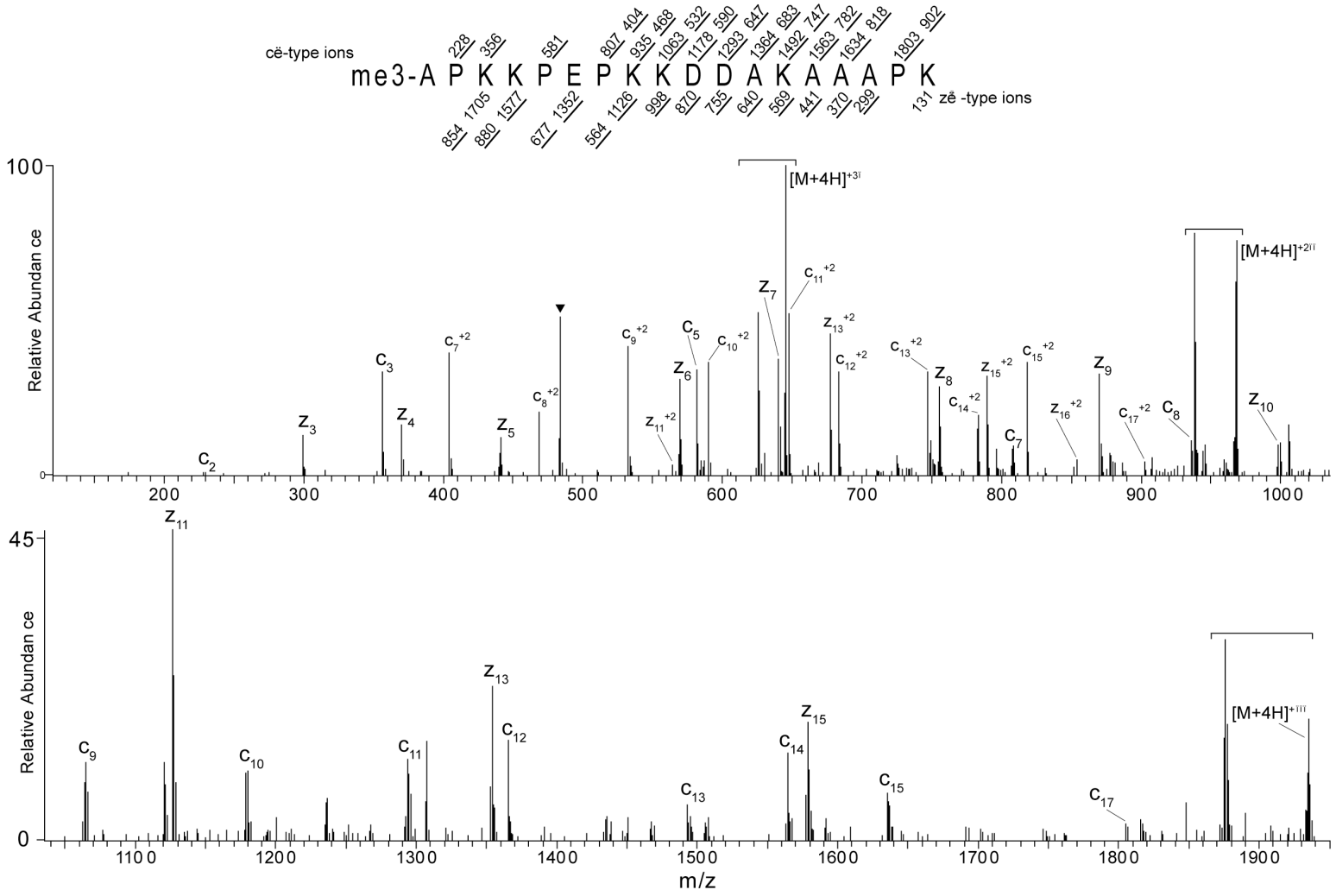

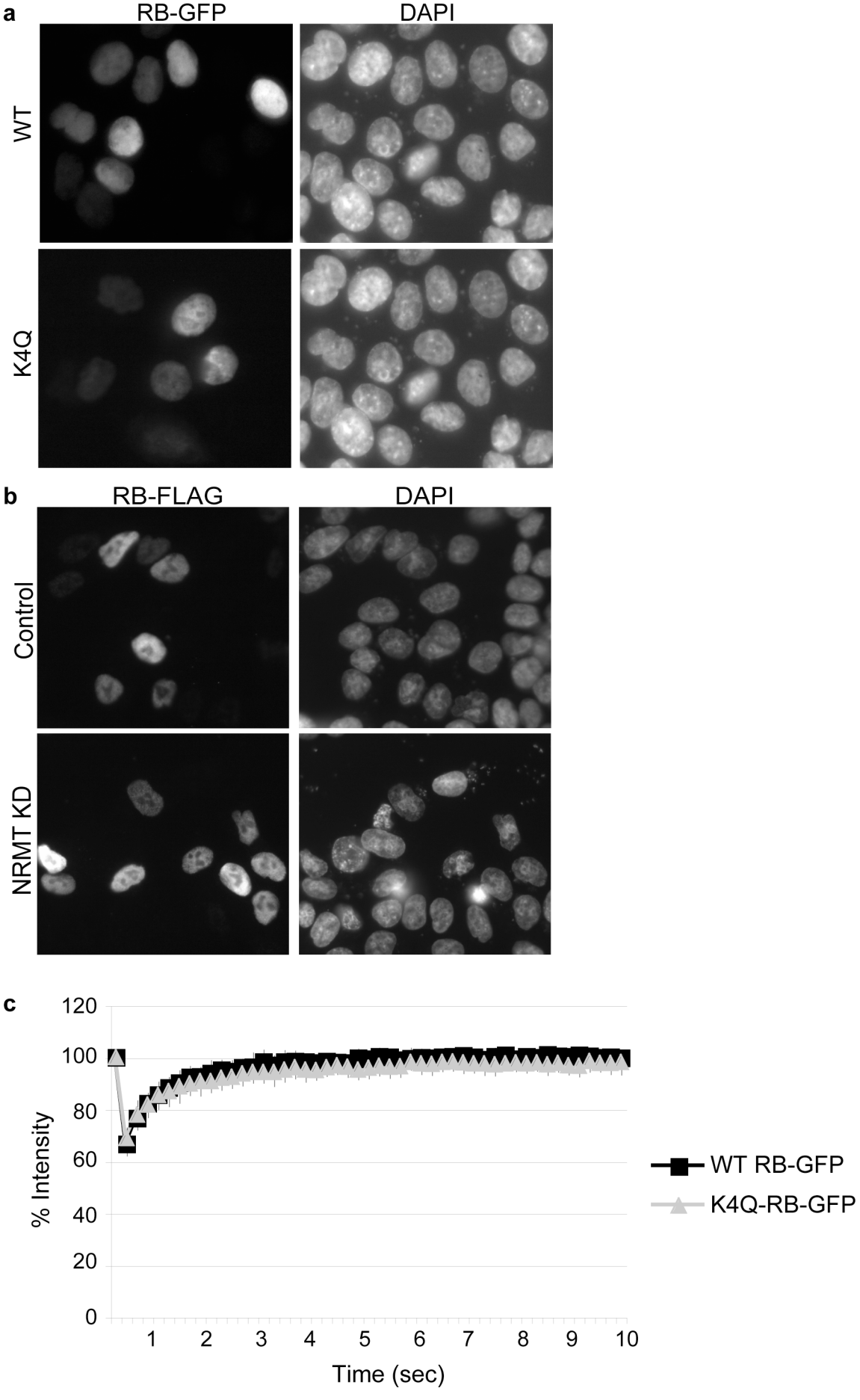
a
RB-GFP
DAPI
WT
K4Q
b
RB-FLAG
DAPI
Control
NRMT KD
c
120
100
80
60
40
20
0
% Intensity
1
2
3
4
5
6
7
8
9
10
Time (sec)
WT RB-GFP
K4Q-RB-GFP